Biochimica et Biophysica Acta 1793 (2009) 335–345

Contents lists available at ScienceDirect

Biochimica et Biophysica Acta

journal homepage: www.elsevier.com/locate/bbamcr

# A large ribonucleoprotein particle induced by cytoplasmic PrP shares striking similarities with the chromatoid body, an RNA granule predicted to function in posttranscriptional gene regulation

Simon Beaudoin, Benoît Vanderperre, Catherine Grenier, Isabelle Tremblay, Frederic Leduc, Xavier Roucou *

*Department of Biochemistry, Faculty of Medicine, University of Sherbrooke, 3001 12ème avenue nord, Sherbrooke, Québec, Canada J1H 5N4*

ARTICLE INFO

*Article history:*
Received 15 May 2008
Received in revised form 23 September 2008
Accepted 14 October 2008
Available online 30 October 2008

*Keywords:*
Prion protein
Chromatoid body
Aggresome
RNA granule
Cytoplasmic prion

ABSTRACT

The observation that PrP is present in the cytosol of some neurons and non-neuronal cells and that the N-terminal signal peptide is slightly inefficient has brought speculations concerning a possible function of the protein in the cytosol. Here, we show that cells expressing a cytosolic form of PrP termed cyPrP display a large juxtanuclear cytoplasmic RNA organelle. Although cyPrP spontaneously forms aggresomes, we used several mutants to demonstrate that the assembly of this RNA organelle is independent from cyPrP aggregation. Components of the organelle fall into three classes: mRNAs; proteins, including the RNAseIII family polymerase Dicer, the decapping enzyme Dcp1a, the DEAD-box RNA helicase DDX6, and the small nuclear ribonucleoprotein-associated proteins SmB/B′/N; and non-coding RNAs, including rRNA 5S, tRNAs, U1 small nuclear RNA, and microRNAs. This composition is similar to RNA granules or chromatoid bodies from germ cells, or planarian stem cells and neurons, which are large ribonucleoprotein complexes predicted to function in RNA processing and posttranscriptional gene regulation. The domain of PrP encompassing residues 30 to 49 is essential for the formation of the RNA particle. Our findings confirm the intriguing relation between PrP and RNA in cells, and underscore an unexpected function for cytosolic PrP: assembling a large RNA processing center which we have termed PrP-RNP for PrP-induced ribonucleoprotein particle.



## 1. Introduction

Prion diseases are a group of transmissible neurodegenerative disorders including Creutzfeldt–Jakob disease (CJD) and Gerstmann–Sträussler–Scheinker syndrome (GSS) in humans, scrapie in sheep and goat, bovine spongiform encephalopathy (BSE) in cattle and chronic wasting disease (CWD) in deer. A common hallmark of prion diseases is the conversion of the cellular prion protein $PrP^{C}$ into $PrP^{Sc}$, a misfolded and proteinase K (PK)-resistant isoform, which is the main component of infectious prions [1–3].

$PrP^{C}$ is primarily a plasma membrane GPI-anchored glycoprotein localized in specialized domains known as lipid rafts [4]. However, besides the major membrane-bound form, $PrP^{C}$ may also be found in transmembrane forms [5,6]. One form, termed $^{Ctm}$PrP, has the COOH-terminus in the ER lumen and the $NH_2$-terminus in the cytosol. The other transmembrane form, termed $^{Ntm}$PrP, has the opposite orientation. Both transmembrane forms appear to span the membrane at the same hydrophobic domain comprised between residues 110 and 135 [7]. Interestingly, progressive neurodegeneration both in GSS syndrome patients with an A117V mutation and in transgenic mice carrying a triple mutation within the hydrophobic domain has been shown to coincide with increased synthesis of $^{Ctm}$PrP [7,8].

The presence of $PrP^{C}$ was also detected in the cytoplasm of different cell types in physiological conditions. $PrP^{C}$ is present in the cytosol in subpopulations of neurons in the hippocampus, neocortex, and thalamus of mice [9]. $PrP^{C}$ is abundantly expressed in the cytoplasm of beta-pancreatic cells from rats and its levels increase in response to hyperglycemia or during normal aging [10]. Hypoxia induces the expression of a GPI-anchorless splice variant of PrP located in the cytosol of a human glioblastoma cell line [11]. This cytosolic variant is also detected in human brains and in non-neuronal tissues [11]. Finally, $PrP^{C}$ is also associated with the sperm cytoplasmic droplets [12]. All together, these results point to a possible role of PrP in the cytoplasm. This hypothesis is supported by the observation that about 20% of PrP never translocates into the ER due to a particularly inefficient ER translocation signal [13].

Based on previous studies, a cytosolic population of PrP would seem disadvantageous since expression of a recombinant PrP without an ER translocation signal is toxic in transgenic animals [14]. This form of PrP is termed cyPrP for clarity purposes. The toxicity of cyPrP in cultured cells is controversial with studies arguing in favour of a

*Abbreviations:* $CyPrP^{EGFP}$, cytoplasmic prion protein genetically fused to EGFP; DDX6, DEAD-box RNA helicase 6; EGFP, enhanced green fluorescent protein; miRNA, microRNA; PrP, prion protein; PrP-RNP, cyPrP-induced RiboNucleoprotein Particle; SmB/B′/N, Small nuclear ribonucleoprotein-associated proteins B/B′/N

* Corresponding author. Tel:. +1 819 346 1110x12248; fax: +1 819 564 5340.
*E-mail address:* xavier.roucou@usherbrooke.ca (X. Roucou).

0167-4889/$ – see front matter © 2008 Elsevier B.V. All rights reserved.
doi:10.1016/j.bbamcr.2008.10.009

noxious function [13–15], and others against [16–18]. Furthermore, only cerebellar cells appeared to be affected in transgenic mice expressing cyPrP [14], suggesting that toxicity may be cell-type dependent.

Recently, we have shown that cells expressing cyPrP spontaneously form PrP aggresomes [19]. Aggresomes are perinuclear organelles where aggregated proteins are centralised. In contrast to other proteins forming aggresomes in cultured cells, PrP aggresomes specifically induce the co-aggregation of mRNAs [20]. Pull down assays using oligo-dT cellulose showed that cyPrP co-purifies with mRNA, indicating that PrP aggresomes are mRNA ribonucleoprotein complexes. In the present study, we have investigated further the relationship between cyPrP and RNA. In addition to mRNA, cyPrP induced the aggregation of various RNA molecules, including U1 small nuclear RNA, 5S ribosomal RNA, and tRNA. In contrast, the distribution of 18S and 28S rRNAs was unchanged. We mapped the RNA aggregation determinant in the N-terminal unstructured domain of PrP. A C-terminal truncated mutant of cyPrP containing the unstructured region of PrP (residues 23–124) and unable to form aggresomes still induced the assembly of a perinuclear RNA organelle. This RNA organelle shares all characteristics of protein aggresomes, including the assembly of a cage of vimentin surrounding the organelle, its localization at the centrosome, and the clustering of mitochondria within the organelle. We used several protein and micro-RNA markers to demonstrate that this RNA organelle is similar to chromatoid bodies from germ-cells, and planarians stem cells and neurons. For clarity purposes, this RNA organelle is termed PrP-RNP for PrP-induced ribonucleoprotein particle. These results reveal a possible function for PrP in the cytoplasm: assembling a specific RNA platform for the storing and processing of RNA.

## 2. Experimental procedures

### 2.1. Antibodies, clones, and reagents

Primary antibodies used were monoclonal anti-Dicer (Abcam, clone 13D6), anti-DDX6 (Abcam, polyclonal 40684), anti-Dcp1a (Abnova, clone 3G4), anti-SmB/B′/N (SantaCruz, polyclonal FL-240), and anti-vimentin (Abcam, clone VI-10 or polyclonal 45939).

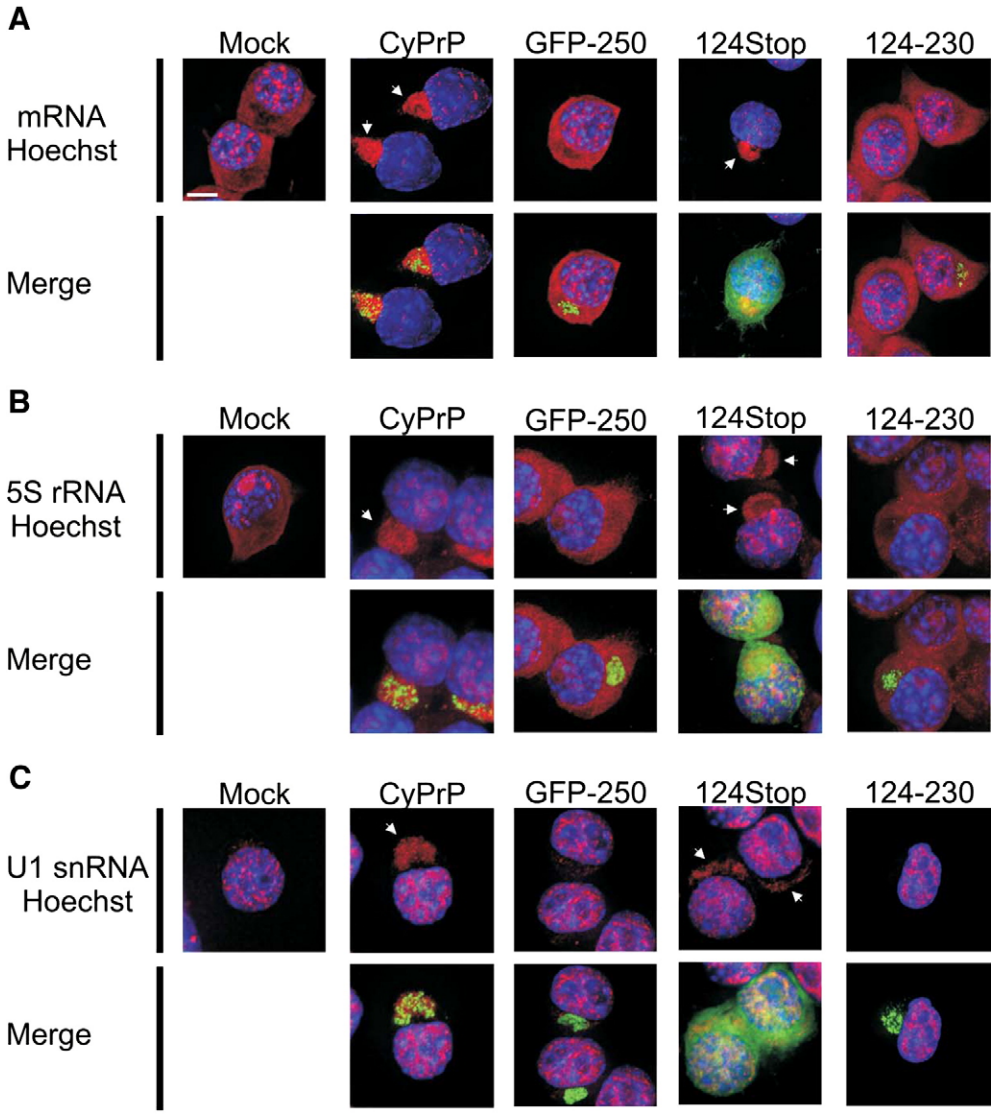


**Fig. 1.** Localization of mRNA, 5S rRNA, U1 snRNA, tRNA, 18S and 28S rRNAs in cells expressing different protein constructs. In situ hybridization was performed with a biotin-labelled oligo(dT) probe to detect mRNAs with a polyA tail (A), or biotin-labelled nucleotide probes specific for 5S rRNA (B), U1 snRNA (C), tRNA (D), 18S rRNA (E), or 28S rRNA (F). N2a cells were either mock-transfected, transfected with $CyPrP^{EGFP}$, GFP-250, $CyPrP^{EGFP}$124stop (124 stop), or $CyPrP^{EGFP}$124–230 (124–230), as indicated. RNA molecules were revealed with alexa568-labelled streptavidin (red), and nuclei were stained with Hoechst (blue). Red and blue channels are shown merged (top panels), and merged with the green channel (bottom panels). White arrows indicate the formation of RNA aggregates. Scale bar: 5 μm. Original magnification ×90.

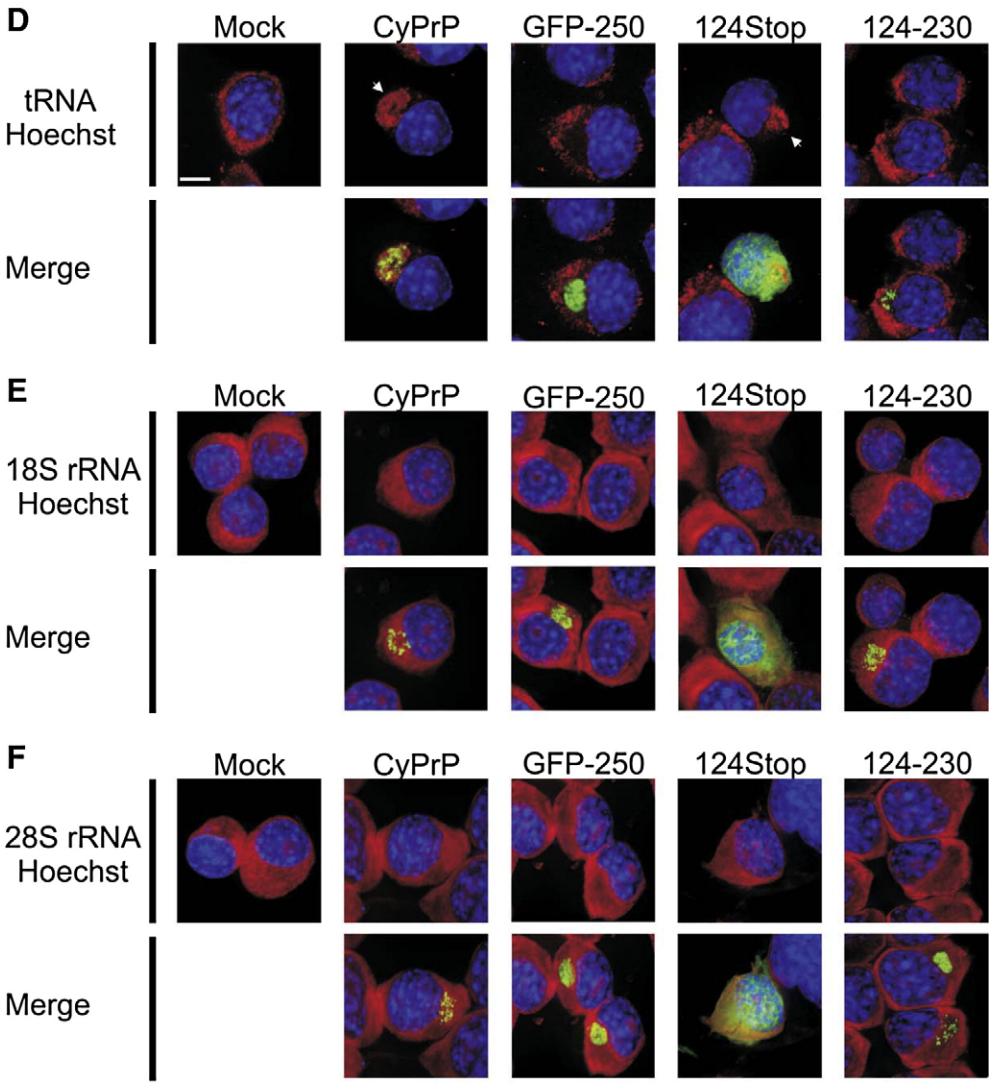


**Fig. 1** (*continued*).

Monoclonal antibody 414 which recognizes five FG-repeat nucleoporins (nup358, nup214/CAN, nup153, nup98, and p62), was purchased from Abcam. Monoclonal SAF32 was purchased from Cayman. Anti-VASA/MVH antibody was a kind gift from Dr Kimmins (McGill University, Montreal, Canada). Secondary antibodies were Alexa Fluor 633 or 568 F(ab′)2 fragment of goat anti-mouse IgG (Invitrogen).

Cloning of CyPrP$^{EGFP}$, CyPrP$^{EGFP}$124stop, and CyPrP$^{EGFP}$124–230 in pCEP4β (Invitrogen) was described previously [19]. CyPrP50–230 was amplified by PCR using forward 5′-cctctcgagctccacctcagggcggtg-3′ and reverse 5′-cgcggatcctcacgatcctctctggtaataggcctg-3′ primers. The PCR product was introduced in the HindIII and BamHI restriction sites of EGFP-pCEP4β [19], to generate CyPrP$^{EGFP}$50–230. CyPrP$^{EGFP}$33–230 was amplified from CyPrP$^{EGFP}$ by PCR using forward 5′-cccaagcttatgaacactgggggcagccgatac-3′ and reverse 5′-cgcggatcctcacgatcctctctggtaataggcctg-3′ primers. The PCR product was introduced in the HindIII and BamHI restriction sites of pCEP4β. CyPrP$^{EGFP}$Δ30-49 was generated from CyPrP$^{EGFP}$ by using the Stratagene Quick Change mutagenesis protocol and the two primers 5′-cgcccgaagcctggaggatggggcaaccgctacccacctcagggc-3′ and 5′-gccctgaggtgggtagcggttgcccccatcctccaggcttcgggcg-3′. Primers were purchased from IDT. All constructs were sequenced in both orientations.

All reagents were obtained from Sigma-Aldrich, unless otherwise stated.

### 2.2. Cell culture, transfections, squash preparations

Mouse N2a neuroblastoma were maintained in Dulbecco's modified Eagle's medium plus 10% fetal bovine serum (Wisent). Transfections were carried out using Exgen according to the manufacturer's protocol (MBI Fermentas).

Testes of adult wild-type C57BL/6 mice were decapsulated in PBS and squash preparations of seminiferous tubules were done as described in [21].

### 2.3. Immunoprecipitation and western blotting

Cells ($10^6$ in 6-well plates) were rinsed twice with 2 ml cold PBS, and lysed with 200 µl buffer A [50 mM Tris–HCl, pH 7.5; 150 mM KCl; 1% NP-40; 1 mM EDTA; 0.5 mM DTT; 1 mini EDTA-free protease inhibitor tablet (Roche) per 10 ml] for 15 min on ice. The lysate was centrifuged at 10,000 ×*g* for 10 min at 4 °C. Twenty µl were kept aside (total input), and the remaining 180 µl were processed for immunoprecipitation. Protein A/G-PLUS-agarose beads (SantaCruz) were mixed for 2 h with 10 µl of anti-vimentin or control isotype antibodies. The antibody-bead mix was then washed with buffer NT2 (50 mM Tris [pH 7.4]; 150 mM NaCl; 1 mM MgCl2; 0.05% Nonindet P-40). Immunoprecipitation was carried out for 12 h at 4 °C. The beads

were then washed three times with 1 ml of buffer NT2, and the bound proteins eluted by incubating for 5 min at 95 °C in SDS-PAGE sample buffer [0.5% SDS (w/v), 1.25% 2-mercaptoethanol (v/v), 4% glycerol (v/v), 0.01% bromphenol blue (w/v), 15 mM Tris–HCl, pH 6.8]. Proteins were detected by western blot using anti-Dicer (1/100), anti-DDX6 (1/1000), anti-Dcp1a (1/500), and anti-SmB/B′/N (1/200) antibodies.

### 2.4. Immunofluorescence, fluorescence in situ hybridization

Cells grown on coverslips were fixed and processed for immunofluorescence as previously described [19]. Primary antibodies dilutions were as followed: Dcp1 (1/100), DDX6 (1/100), Dicer (1/100), SmB/B′/N (1/50), VASA/MVH (1/200). Secondary antibodies were diluted 1/1000.

For in situ staining, permeabilized cells were incubated 10 min with 2 × SSC, and hybridized with 1 nM of an end-labelled biotinylated probes overnight at 10 °C below the Tm in the hybridization mixture (2 × SSC, 1 mg/ml yeast tRNA, 10% dextran sulphate, 25% formamide). Probes were specific for mRNAs (oligo-dT20),U1 (5′-aaaaccaccttcgtgatcatggtatctcccc-3′), 5S rRNA (5′-tattcccaggcggtctcccatccaagtactaac-3′), 18S rRNA (5′-atatacgctattggagctggaattacc-3′), 28S rRNA (5′-agtgggtgaacaatccaacgcttgg-3′), let-7a (5′-aactatacaacctactacctca-3′), miR21 (5′-tcaacatcagtctgataagcta-3′), miR122a (5′-caaacaccattgtcacactcca-3′), and tRNA-Leu-CAG (5′-aagtccagcgtcagagggga-3′). tRNA-Leu-CAG was chosen because it is the most abundant in cells. All of the probes were purchased from IDT. After washing twice with 2 × SSC and once with 0.5 × SSC, cells were equilibrated in 1 × PBS containing 1 mg/ml BSA. Cells were incubated with 2 μg/ml Alexa Fluor 633-labelled streptavidin (Molecular Probes) in 1 × PBS containing 1 mg/ml BSA. After a 1 h incubation, cells were washed and mounted as previously described [10].

In the in situ staining protocol of squash preparations, the hybridization mixture contained 0.2 mg/ml BSA.

### 2.5. Microscopy

For epifluorescence analysis, cells were examined with an Eclipse TE2000-E visible/epifluorescence inverted microscope (Nikon Corporation, Japan) equipped with band pass filters for fluorescence of Hoechst (Ex. D340/40: Em. D420), GFP (Ex. D450/40: Em. D500/50) and tetramethylrhodamine isothiocyanate (TRITC) (Ex. D528/25: Em. D590/60) (Nikon Corporation). Photomicrographs of 1344 × 1024 pixels were captured using either 60× or 100× oil immersion objectives and Orca cooled color digital camera (Hamamatsu Photonics, Japan). Images were processed using NIS Elements AR software (Nikon Corporation). Within the same figure, all pictures were taken with the same exposure time.

For confocal analysis, cells were examined with a scanning confocal microscope (FV1000, Olympus, Tokyo, Japan) coupled to an inverted microscope with a 63× oil immersion objective (Olympus). Specimens were laser-excited at 488 nm (40 mW Argon laser) and 633 nm (Helium–Neon laser). In order to avoid cross-talk between the emitted EGFP and Alexa Fluor 633 fluorescences were collected sequentially at wavelengths 525–550 and >590 nm respectively. Serial horizontal optical sections of 512×512 pixels with 2 times line averaging were taken at 0.11 μm intervals through the entire thickness of the cell (optical resolution: lateral −0.18 μm; axial −0.25 μm). Images were acquired during the same day, typically from 5 cells of similar size from each experimental condition using identical settings of the instrument. For illustration purposes images were pseudocolored according to their original fluorochromes, merged (FluoView

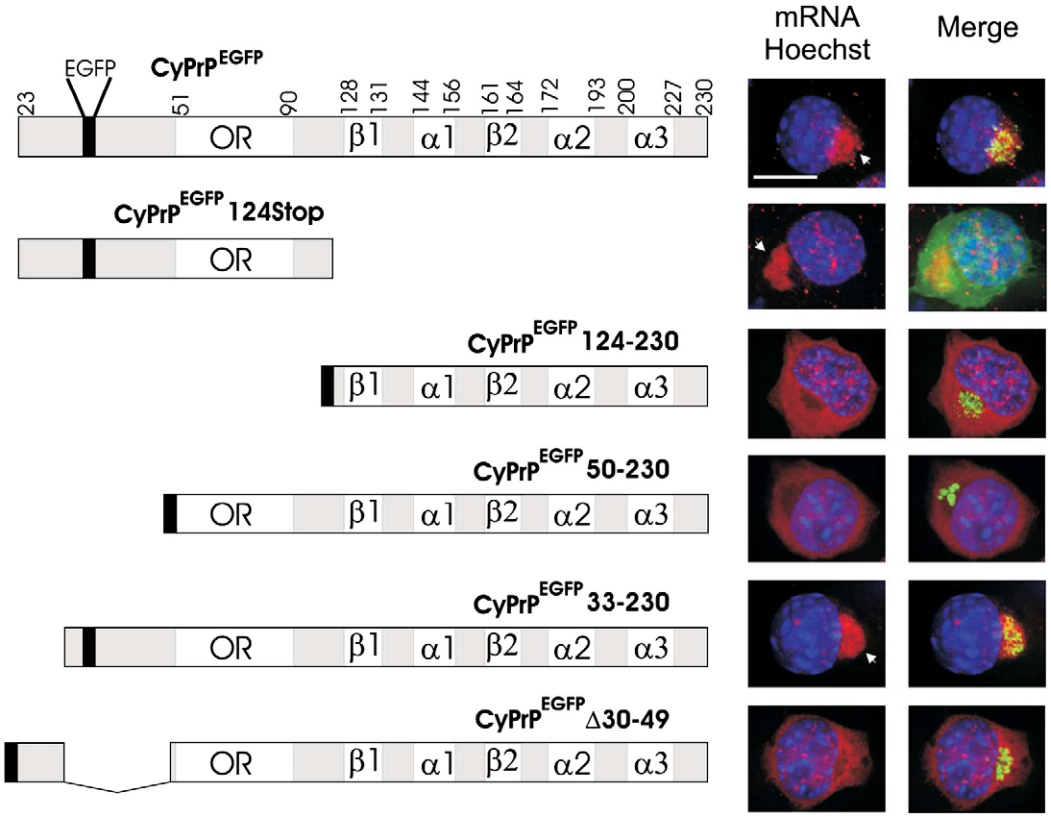


**Fig. 2.** The domain located between residues 30 and 49 is necessary for the assembly of PrP-RNP. Diagrams of CyPrP$^{EGFP}$ and several deletion mutants engineered in this study are represented. Numbers indicate residues at the junction of different structural domains (adapted from [51]). Black box represents EGFP coding sequence. The formation of PrP-RNPs was evaluated by in situ hybridization with a biotin-labelled oligo(dT) probe and alexa568-labelled streptavidin to detect mRNAs (red). Nuclei were stained with Hoechst (blue). Red and blue channels are shown merged (left panels), and merged with the green channel (right panels). White arrows indicate PrP-RNPs. Scale bar: 10 μm. Original magnification ×90.

software, Olympus), then cropped and assembled (Adobe Photoshop software, Adobe Systems, Mountain View, CA).

## 3. Results

### *3.1. Co-aggregation of 5S, U1, tRNA but not 18S and 28S with PrP aggresomes*

The observation that mRNAs aggregate with PrP aggresomes prompted us to investigate the specificity of this co-aggregation [20]. We performed fluorescence in situ hybridization (FISH) using probes specific for various RNA molecules, including ribosomal 5S, 18S, and 28S RNAs, the small nuclear U1 RNA, and tRNAs. Fluorescent PrP aggresomes were reconstituted by expressing cyPrP$^{EGFP}$ in murine neuroblastoma N2a cells [19,20]. The analysis on N2a cells expressing cyPrP$^{EGFP}$ revealed a concentration of mRNA, 5S, U1, and tRNA with PrP aggresomes (Fig. 1A–D). In contrast, 18S and 28S rRNAs did not co-aggregate with PrP aggresomes, but remained diffuse in the cytoplasm and the nucleoli (Fig. 1E, F). Previously, we showed that aggregation of mRNAs was specific to PrP aggresomes since the aggresome-forming protein GFP-250 used as a model to study the dynamics of protein aggresomes did not display any mRNA clustering activity [20] (Fig. 1A).

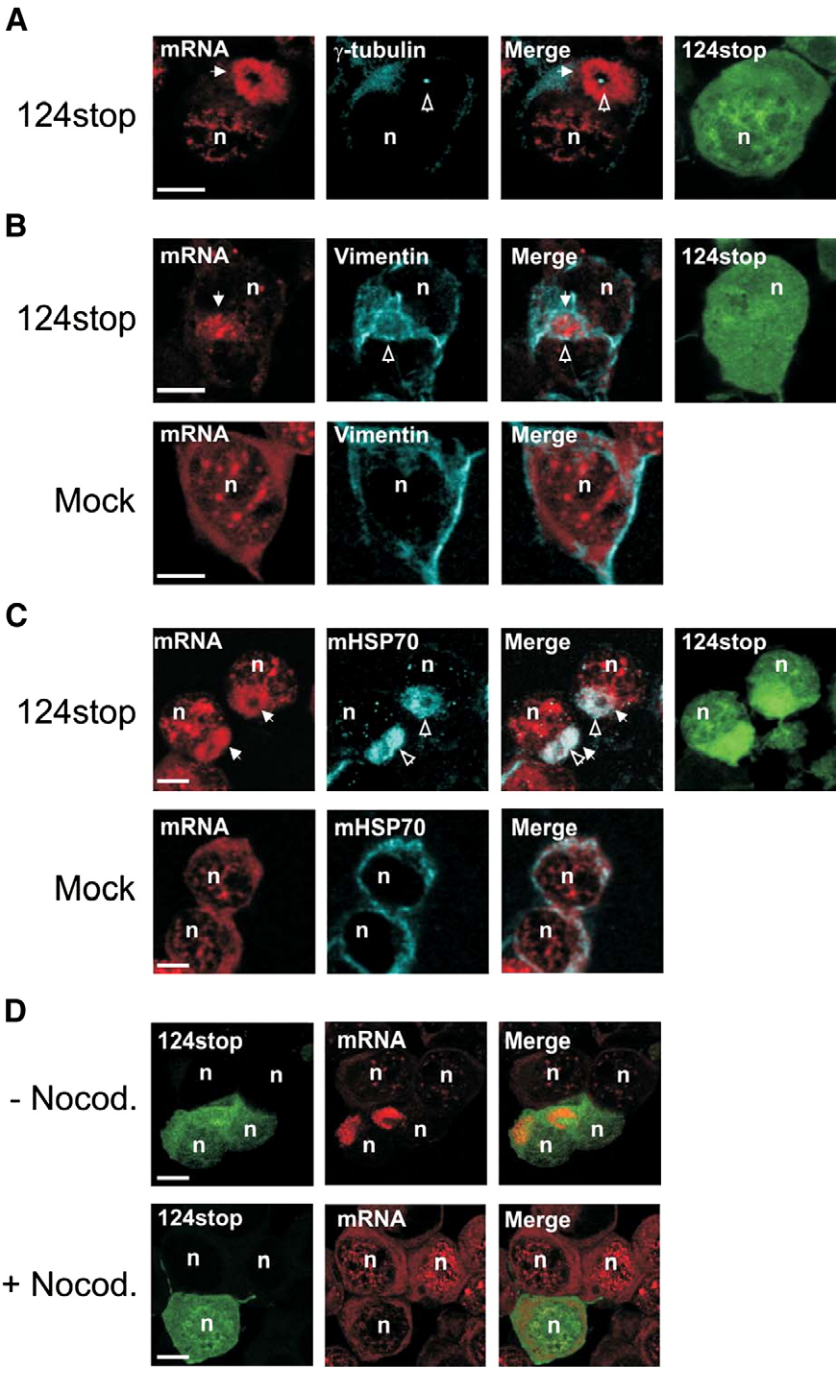


**Fig. 3.** Aggresomal characteristics of PrP-RNPs. Confocal analysis of γ-tubulin (A), vimentin (B), and mtHSP70 (C) (cyan channel) in mock-transfected N2a cells or in cells transfected with CyPrP$^{EGFP}$124stop (green channel), as indicated. PrP-RNPs (white arrows) were detected by in situ hybridization with a biotin-labelled oligo(dT) probe and alexa633-labelled streptavidin (red). Red and cyan channels are shown merged. N, nucleus. Empty arrows indicate the centrosome (A), the cage of vimentin (B), and the clustering of mitochondria (C). (D) Distribution of mRNA in cells incubated for 12 h in the presence of nocodazole (10 μg/ml). Cells were transfected with CyPrP$^{EGFP}$124stop 12 h prior to the addition of nocodazole. Scale bar: 5 μm. Original magnification ×60.

Similarly, aggregation of 5S, U1, and tRNA was specific to PrP aggresomes since GFP-250 did not modify their intracellular distribution (Fig. 1B–D). As expected, the formation of GFP-250 aggresomes did not alter the distribution of 18S and 28S rRNAs (Fig. 1E, F). These results indicate that several but not all RNA molecules co-aggregate specifically with PrP aggresomes.

### 3.2. Cytosolic PrP can induce the aggregation of RNA independently of the formation of aggresomes

CyPrP$^{EGFP}$ co-purifies with mRNAs in oligo-dT cellulose pull down assays, strongly suggesting that PrP aggresomes are in fact poly(A)$^+$ ribonucleoprotein complexes [20]. This hypothesis predicts that aggregation of cyPrP$^{EGFP}$ should be essential for the assembly of ribonucleoprotein complexes. In order to address this issue, we used a mutant unable to form aggresomes, cyPrP$^{EGFP}$124stop [19]. This mutant contains the unstructured N-terminus of PrP (residues 23–124). Strikingly, mRNAs still assembled in a large juxtanuclear organelle in cells expressing cyPrP$^{EGFP}$124stop (Fig. 1A). This observation was confirmed with probes specific to 5S, U1, and tRNAs (Fig. 1B–D). Similar to cyPrP$^{EGFP}$, 18S and 28S rRNAs did not aggregate in cells expressing cyPrP$^{EGFP}$124stop (Fig. 1E, F).

In additional experiments, we expressed CyPrP$^{EGFP}$124–230, a protein construct representing the C-terminal structured domain of PrP which forms aggresomes [19]. As expected, cells expressing cyPrP$^{EGFP}$124–230 assembled aggresomes; however, cyPrP$^{EGFP}$124–230 aggresomes did not modify the distribution of RNAs (Fig. 1). Thus, aggregation of mRNAs, 5S rRNA and U1 snRNA is independent from the aggregation of cyPrP. In addition, residues responsible for the formation of this RNA organelle lie in the N-terminal domain of cyPrP.

Since the aggregation of cyPrP is not essential for the assembly of the RNA organelle and that this organelle also contains proteins (below), we termed this organelle PrP-induced ribonucleoprotein particle or PrP-RNP. Several deletion mutants containing the C-terminal domain and thus capable of forming protein aggresomes were engineered to precisely map the domain of PrP in the N-terminal region that signals the formation of PrP-RNPs (Fig. 2). PrP-RNPs were not formed in cells expressing CyPrP$^{EGFP}$50-230 but assembled in cells expressing CyPrP$^{EGFP}$33–230, indicating that the aggregation determinant of PrP-RNPs was located between residues 33 and 50. This was confirmed by expressing CyPrP$^{EGFP}$Δ30–49, a deletion mutant missing a domain located between residues 30 to 49. This mutant was not able to induce the formation of PrP-RNP (Fig. 2).

### 3.3. PrP-RNPs share structural and functional criterions similar to protein aggresomes

PrP-RNPs, like protein aggresomes, assemble in a juxtanuclear area. One possibility to explain this observation would be that these RNA organelles are in fact RNA-containing aggresomes. To test this hypothesis, we examined four main features of protein aggresomes in cells expressing cyPrP$^{EGFP}$124stop; localization of PrP-RNPs around the microtubule organising center or centrosome, assembly of a cage of vimentin around PrP-RNPs, clustering of mitochondria, and the requirement for an intact microtubule network for their assembly [22]. As shown in Fig. 3A and B, PrP-RNPs also localized around γ-tubulin, a component of the centrosome, and were surrounded by a cage composed of vimentin protein. Furthermore, a major rearrangement of the mitochondrial network occurred in cells expressing cyPrP$^{EGFP}$124stop. Mitochondria, which are normally distributed throughout the cytoplasm were clustered around PrP-RNPs, leaving no detectable mitochondria in other regions of the cytoplasm (Fig. 3C). We also tested the effect of the microtubule-depolymerising agent nocodazole. Nocodazole completely prevented the formation of PrP-RNPs (Fig. 3D). Thus, besides cytological criterions examined above, PrP-RNPs also share functional features with protein aggresomes.

### 3.4. PrP-RNPs and RNA granules from germ cells or planarian stem cells and neurons share similar components

To our knowledge, the only known cytoplasmic bulky RNA particle described in the literature is large, nonmembranous, RNA-rich organelles typically found around the nuclei of germ cells, planarian stem cells and neurons [23,24]. Germ granules are also known under the name of chromatoid bodies [25]. Similar to PrP-RNPs, chromatoid bodies contain mRNAs, 5S rRNA and U1 snRNPs [26,27]. They also display aggresomal characteristics, including a cage of vimentin surrounding the RNA granule [28]. mRNA is the only RNA molecule that has been detected by FISH in chromatoid bodies; the presence of 5S was detected by electrophoretic analysis of RNA extracted from chromatoid bodies, and the presence of 18S and 28S was not sought [26]. Furthermore, the presence of U1 was indirectly detected using anti-U1 snRNP antibodies [27]. In order to compare the RNA

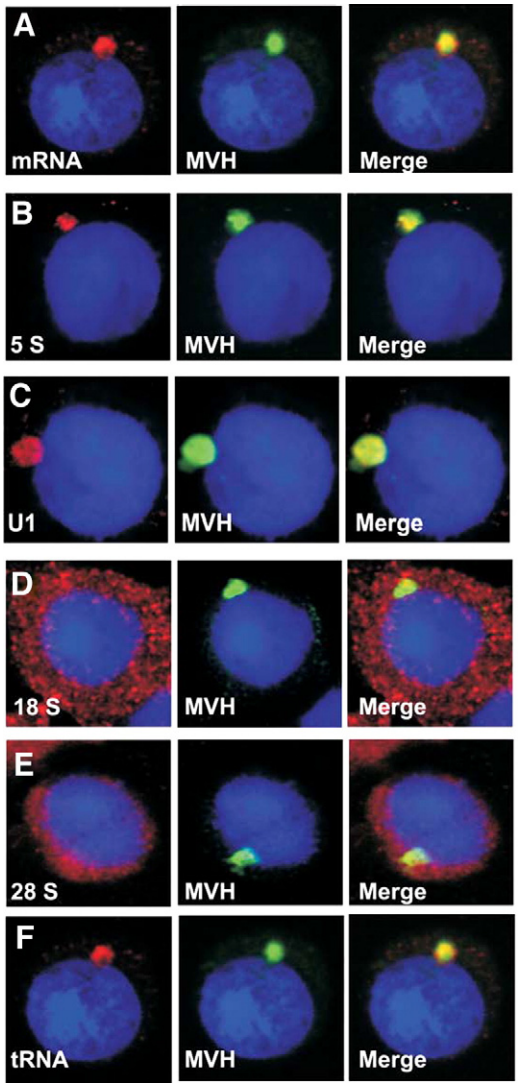


**Fig. 4.** Localization of different RNAs in chromatoid bodies by in situ hybridization and confocal microscopy. Squashed samples from stages V–VII mouse seminiferous tubules were used. In situ hybridization was performed with a biotin-labelled oligo(dT) probe to detect mRNAs (A), or biotin-labelled nucleotide probes specific for 5S rRNA (B), U1 snRNA (C), 18S rRNA (D), 28S rRNA (E), or tRNA (F) (red channel). RNA molecules were revealed with alexa633-labelled streptavidin (red). After in situ hybridization, VASA homolog MVH signals were detected by immunofluorescence (green channel), and nuclei were stained with Hoechst (blue channel). Scale bar: 5 μm. Original magnification ×60.

composition of PrP-RNPs and chromatoid bodies, we performed FISH experiments on squash preparations of mouse seminiferous tubules. The ATP-dependent DEAD-box RNA helicase VASA/MVH was used as a specific marker for the chromatoid body [29,30]. The chromatoid body was labelled with poly($A^+$), 5S and U1 probes (Fig. 4A–C). In contrast, there was no concentration of 18S and 28S rRNAs in the chromatoid body (Fig. 4D, E). Interestingly, tRNAs were also concentrated in chromatoid bodies although some tRNA remained distributed throughout the cytoplasm (Fig. 4F).

These data motivated us to further analyze a possible relationship between chromatoid bodies and PrP-RNPs. Recently, several miRNAs were shown to concentrate in chromatoid bodies, including miR-122a, miR-21, and let-7a [30]. The distribution of these miRNAs was determined by FISH using specific oligonucleotide probes in cells expressing cyPrP$^{EGFP}$ and cyPrP$^{EGFP}$124stop. In agreement with previous studies, miRNAs were mostly located throughout the cytoplasm in control untransfected cells (Fig. 5) [31,32]. The analysis on cells expressing cyPrP$^{EGFP}$ revealed a high concentration of miR-122a, miR-21, and let-7a within PrP-RNPs. miRNAs also concentrated in a juxtanuclear area in cells expressing cyPrP$^{EGFP}$124stop (Fig. 5).

Chromatoid bodies are also characterized by the accumulation of a specific set of proteins [25]. Here, four different protein markers were investigated in cells expressing cyPrP$^{EGFP}$124stop. Similar results were obtained in cells expressing cyPrP$^{EGFP}$ (not shown). First, the mRNAs decapping Dcp1a enzyme is a component of RNA processing bodies or P-bodies and has normally a granular cytoplasmic localization [33]. Interestingly, Dcp1a concentrate in chromatoid bodies, indicating a functional analogy with P-bodies [30]. The granular distribution of Dcp1a was confirmed in mock-transfected cells (Fig. 6A). In sharp contrast, Dcp1a concentrate in PrP-RNPs (Fig. 6B). Second, the DEAD box-family RNA helicase VASA/MVH is a classical marker of chromatoid bodies [29,30]. VASA/MVH is specific to germinal cells and could not be detected in N2a cells (not shown). We determined if DDX6, a more ubiquitous DEAD box RNA helicase generally present in messenger ribonucleoprotein particles including P-bodies and stress granules could concentrate in PrP-RNPs [34,35]. Indeed, DDX6 accumulated in PrP-RNPs in cells expressing cyPrP$^{EGFP}$124stop (Fig. 6C, D). Third, Dicer, a double-stranded RNAseIII essential for RNA interference and the biogenesis of miRNAs was recently detected in chromatoid bodies [30]. It was suggested that chromatoid bodies may participate in the posttranscriptional control of gene expression through the small RNAs pathway [30]. Remarkably, we also found Dicer associated with PrP-RNPs (Fig. 6E, F). Finally, Sm proteins are essential core components of small nuclear ribonucleoprotein particles present in the spliceosome. Sm proteins are central to RNA metabolism, and are involved in diverse processes such as pre-mRNA splicing and telomere formation. Sm proteins also localize to the chromatoid body [27,36]. Using an antibody recognizing the three Sm proteins B/B′/N, Sm proteins were also detected in PrP-RNPs (Fig. 6G, H).

In a control experiment, we verified that the concentration of proteins in PrP-RNPs is not a general phenomenon. Previously, we have shown that ribosomal protein S6 did not co-aggregate with mRNA in cyPrP$^{EGFP}$ aggresomes [20]. Ribosomal protein S6 does not coalesce in PrP-RNPs either but remains distributed throughout the cytoplasm (Fig. 6I, J).

### 3.5. PrP-RNPs and nuclear pore complexes

One important feature of chromatoid bodies is their frequent contacts with nuclear pore complexes [37]. In some instances, material continuities between intranuclear dense particles and chromatoid bodies are revealed by electron microscopy. In order to verify the relationship between nuclear pore complexes and PrP-RNPs, nuclear pores were immunostained using antibodies against FXFG repeat nucleoporins, which are positioned throughout the pore complexes. Indirect immunofluorescence images combined with FISH with an oligo-dT probe confirmed the proximity between PrP-RNPs and the nuclear envelope in cells expressing cyPrP$^{EGFP}$ or cyPrP$^{EGFP}$124stop (Fig. 7A). Furthermore, similar to chromatoid bodies, some FXFG repeat nucleoporins were also present in PrP-RNPs (Fig. 7A).

An important characteristic of the chromatoid body is its movements along and perpendicular to the nuclear envelope [37]. PrP-RNPs were mainly detected close to the nuclear pore complexes, but were also detected at a variable distance from the nuclear envelope (compare Fig. 7A and B).

### 3.6. Association between vimentin and protein components of PrP-RNPs

To biochemically confirm the assembly of PrP-RNPs, we attempted to affinity-purify protein components of this organelle using vimentin

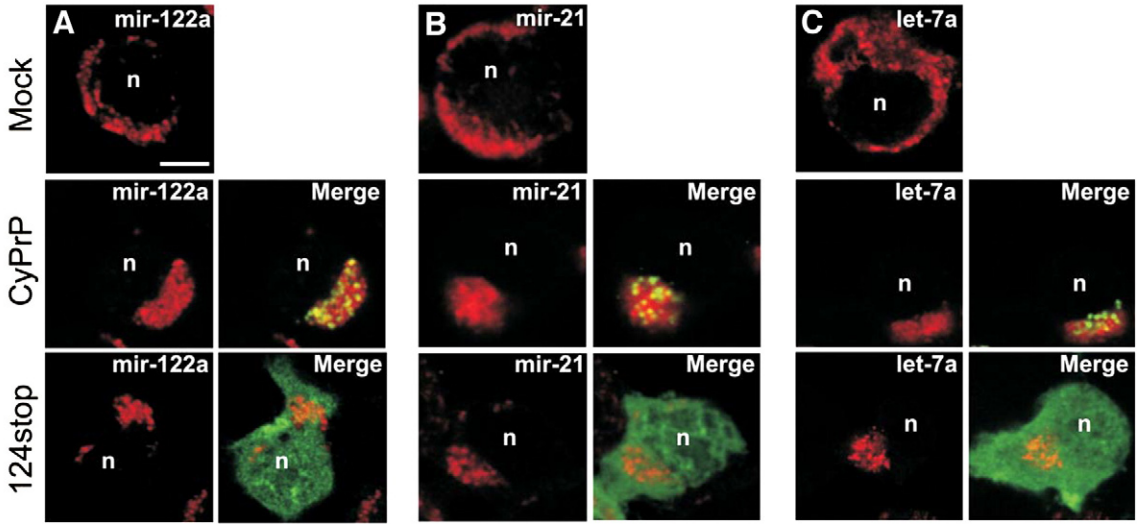


**Fig. 5.** miRNAs are concentrated in PrP-RNPs. Biotin-labelled nucleotide probes specific for miR-122a (A), miR-21 (B), and let-7a (C) were used to determine the distribution of miRNAs in mock-transfected N2a cells, or cells transfected with CyPrP$^{EGFP}$ or CyPrP$^{EGFP}$124stop (green channel), as indicated. The miRNAs were revealed by confocal microscopy with alexa568-labelled streptavidin (red channel). N, nucleus. Scale bar: 5 μm. Original magnification ×60.

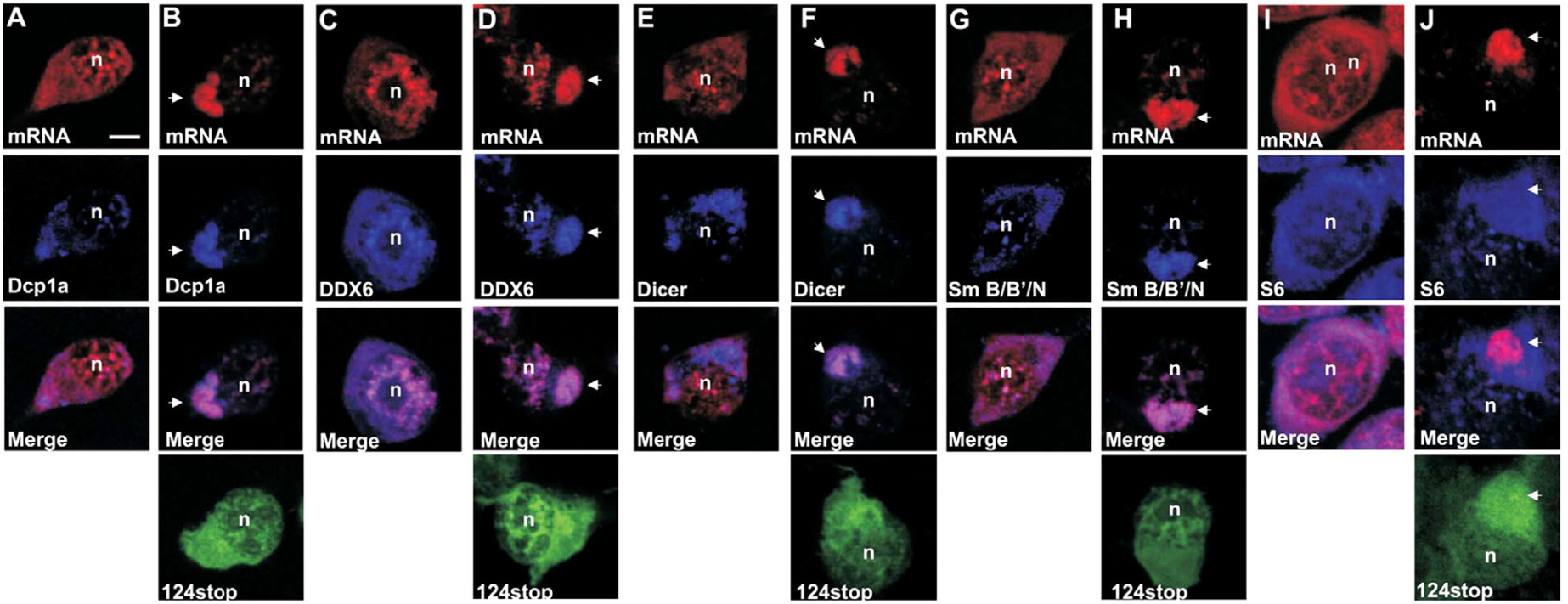


**Fig. 6.** Localization of Dcp1a, DDX6, Dicer, and SmB/B′/N in PrP-RNPs by confocal microscopy. PrP-RNPs (arrows) were revealed by in situ hybridization with a biotin-labelled oligo(dT) probe to detect mRNAs (red channel) in mock-transfected N2a cells (A, C, E, G, I) or N2a cells expressing $CyPrP^{EGFP}$124stop (green channel in B, D, F, H, J). Following in situ hybridization, Dcp1a (A, B), DDX6 (C, D), Dicer (E, F), SmB/B′/M (G, H), and ribosomal S6 protein (I, J) were detected by immunofluorescence using specific antibodies (blue channel). n, nuclei. Arrows show PrP-RNPs. Scale bar: 5 μm. Original magnification ×60.

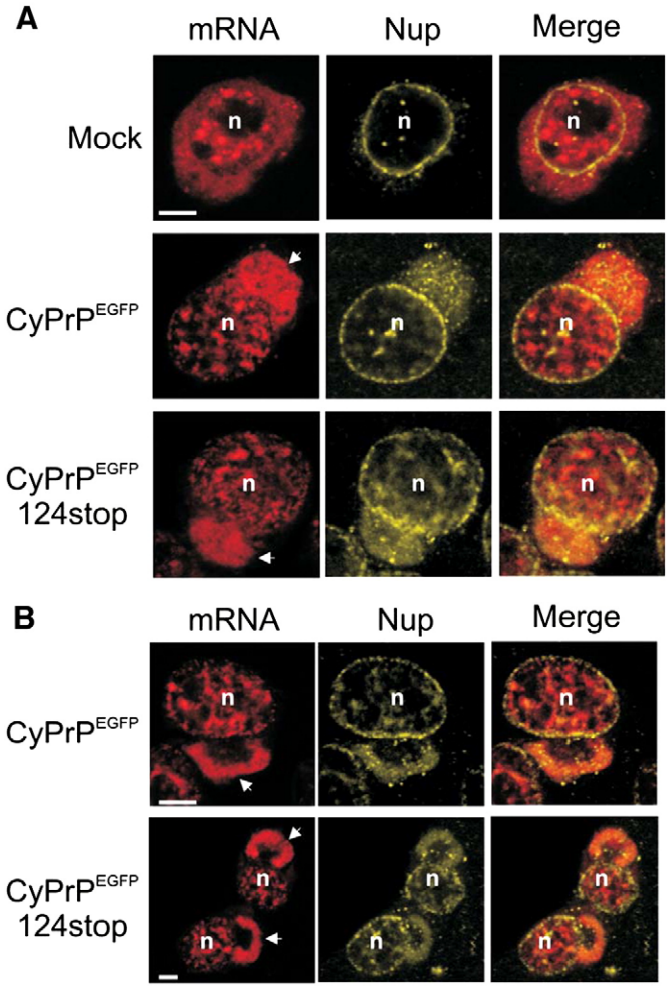


**Fig. 7.** PrP-RNPs are proximal to the nuclear envelope and contain FXFG repeat nucleoporins. Confocal images of PrP-RNPs revealed by in situ hybridization with a biotin-labelled oligo(dT) probe and alexa633-labelled streptavidin to detect mRNAs (red channel) in mock-transfected N2a cells, or in N2a cells expressing CyPrP$^{EGFP}$ or CyPrP$^{EGFP}$124stop, as indicated. Following in situ hybridization, FXFG repeat nucleoporins (Nup) were detected by immunofluorescence using specific antibodies (yellow channel). (A) PrP-RNPs are mainly located in close contact to the nuclear envelope. (B) PrP-RNPs may also be observed far from the nuclear envelope. (A, B) Some FXFG repeat nucleoporins are detected within PrP-RNPs. n, nuclei. Arrows show PrP-RNPs. Scale bar: 5 μm. Original magnification ×60.

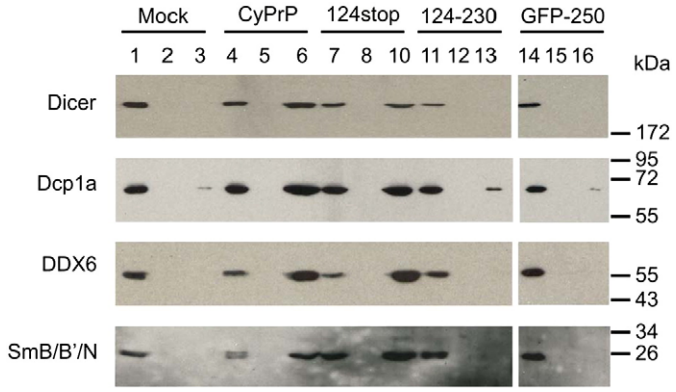


**Fig. 8.** Association of PrP-RNPs and vimentin. Co-immunoprecipitation experiments with anti-vimentin antibodies were performed using mock-transfected N2a cells (lanes 1–3), or N2a cells transfected with CyPrP$^{EGFP}$ (lanes 4–6), CyPrP$^{EGFP}$124stop (lanes 7–10), CyPrP$^{EGFP}$124–230 (lanes 11–13), or GFP-250 (lanes 14–16). Lanes 1, 4, 7, 11, 14 show Dicer, Dcp1, DDX6, and SmB/B′/N in 5% of total cell lysate. Lanes 2, 5, 8, 12, and 15 show affinity-purified Dicer, Dcp1, DDX6, and SmB/B′/N using isotype control antibodies. Lanes 3, 6, 8, 13, and 16 show affinity-purified Dicer, Dcp1, DDX6, and SmB/B′/N using anti-vimentin antibodies. Molecular weight markers in kDa are indicated on the right. This experiment is representative of three independent experiments.

antibody-coated protein A/G sepharose beads. Immunoprecipitates from cells expressing cyPrP$^{EGFP}$ or cyPrP$^{EGFP}$124stop contained Dcp1a, DDX6, Dicer, and Sm (Fig. 8, lanes 6, 10). In contrast, these proteins did not purify with anti-vimentin antibodies in mock-transfected cells, confirming the specificity of this association in cells with PrP-RNPs (Fig. 8, lane 3). We consistently observed some association between vimentin and Dcp1a. However, this association was largely increased in cells expressing cyPrP$^{EGFP}$ or cyPrP$^{EGFP}$124stop (Fig. 8). Isotype control antibody did not immunoprecipitate Dcp1a, DDX6, Dicer, and SmB/B′/N, again confirming the specificity of this interaction (Fig. 8, lanes 5, 8). Furthermore, anti-vimentin antibodies did not purify Dcp1a, DDX6, Dicer, and SmB/B′/N in cells expressing CyPrP$^{EGFP}$124–230 (lanes 11–13), or GFP-250 (14–16).

### *3.7. PrP is detected in the cytoplasm of mouse germ cells displaying a chromatoid body*

Chromatoid bodies are absent in spermatocytes before the second meiosis of spermatogenesis, and are visible in round spermatids during the haploid phase of spermatogenesis [37]. They disappear with the residual body during late spermatogenesis. In order to test the hypothesis that endogenous PrP may be present in the cytoplasm of round spermatids, we analyzed the distribution of PrP in germ cells before the second meiosis and during the haploid phase in squash preparations of mouse seminiferous tubules (Fig. 9). PrP is mainly located at the plasma membrane in spermatocytes (Fig. 9A). In contrast, PrP has a cytoplasmic distribution in round spermatids containing a chromatoid body (Fig. 9B).

## 4. Discussion

The presence of PrP in the cytosol has been detected in a subpopulation of neurons and in beta-pancreatic cells [9,10]. A recent study described a new GPI-anchorless splice variant of the prion

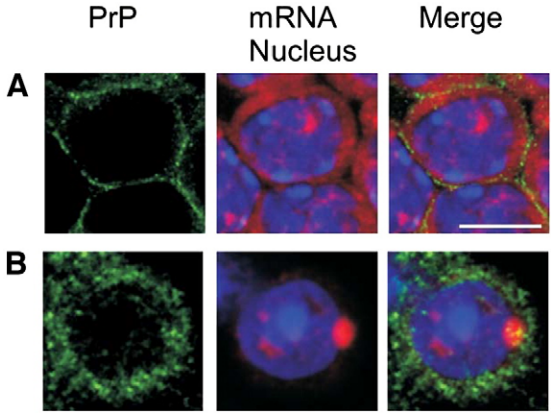


**Fig. 9.** Cytoplasmic localization of endogenous PrP in germ cells containing a chromatoid body. Confocal images of squashed samples from pachitene stage (before second meiosis, A) and haploid stage (B) of mouse seminiferous tubules. Squashed samples are fixed and permeabilized. In situ hybridization was performed with a biotin-labelled oligo(dT) probe to detect mRNAs. mRNAs were revealed with alexa633-labelled streptavidin (red). After in situ hybridization, endogenous PrP signals were detected by immunofluorescence (SAF32 antibody, green channel), and nuclei were stained with Hoechst (blue channel). PrP was not detected at the plasma membrane in cells from haploid stages (B). Scale bar: 5 μm. Original magnification ×60.

protein in human brain and non-neuronal tissues [11]. Interestingly, this variant is located in the cytosol and its levels increase in hypoxic conditions in a human glioblastoma cell line. Altogether, these results point to a possible function of PrP in the cytoplasm. Yet, whether PrP has a specific function in this location and what this function might be has remained elusive. Our findings support a scenario where cyPrP induces the assembly of an RNA processing center similar to RNA granules termed chromatoid bodies.

### *4.1. cyPrP induces the assembly of a large ribonucleoprotein particle termed PrP-RNP*

An important result of this study is the observation that cyPrP induces the formation of an RNA organelle termed PrP-RNP. We have also observed PrP-RNPs in several neuronal and non-neuronal cells from murine and human origin. In this manuscript, only results obtained in N2a cells are shown for clarity reasons. The composition of PrP-RNPs is not specific to one class of RNA but includes several types of RNA molecules. These results seem to be in accordance with previous in vitro studies describing the nucleic-acid binding activity of recombinant PrP [38]. If co-aggregation of cyPrP and RNA is a consequence of a direct interaction between these two macromolecules, a strict correlation should be expected between cyPrP aggregation and the assembly of PrP-RNPs. Hence, aggregation of cyPrP should be essential for the assembly of PrP-RNPs. However, expression of several deletion mutants demonstrates that aggregation of cyPrP and RNA can be uncoupled. Similar to PrP aggresomes, PrP-RNPs induced by a cyPrP mutant unable to aggregate deposit at the centrosome, are surrounded by a cage of vimentin, and their assembly is dependent on a functional microtubule network. Thus, cyPrP and PrP-RNPs co-aggregate for the reason that they utilize the same aggresomal pathway.

These results are significant in terms of the molecular activity of cyPrP. They show that in the cytosol, PrP activates an aggresomal pathway responsible for the biogenesis of PrP-RNPs. This activity is independent from cyPrP aggregation and therefore, does not require a direct contact between cyPrP and RNA in the PrP-RNP. However, the possibility that an interaction between cyPrP and a specific RNA molecule may be responsible for the induction of PrP-RNPs cannot be ruled out. In favour of this hypothesis, the domain involved in the assembly of PrP-RNPs is located between residues 30 and 50; interestingly, this domain also binds RNA in vitro [39].

### *4.2. PrP-RNPs are similar to chromatoid bodies*

Although several types of RNAs concentrate in PrP-RNPs, the observation that cyPrP does not modify the distribution of 18S and 28S rRNAs indicates some specificity and regulation in the mechanism of assembly of PrP-RNPs. Several lines of evidence suggest that PrP-RNPs are similar to previously described RNA granules also known as chromatoid bodies from germ cells, or from planarian stem cells and neurons [25,36]. First, both organelles concentrate identical RNA molecules. We used FISH to confirm the presence of mRNA, snU1RNA, 5S rRNA, and several miRNAs in spermatid cells and in PrP-RNPs. We could also detect tRNAs in these RNA granules. Second, proteins involved in different steps of the metabolism of RNA and that accumulate in chromatoid bodies also concentrate in PrP-RNPs. Third, like chromatoid bodies, PrP-RNPs share similar aggresomal characteristics. Fourth, similar to chromatoid bodies, PrP-RNPs are proximal to nucleoporins. Fifth, endogenous PrP is present in the cytoplasm of round spermatids containing chromatoid bodies. Despite these characteristics, the possibility that PrP-RNPs and chromatoid bodies are different organelles cannot be completely excluded.

It has become generally accepted that assembly of the chromatoid body constitutes a mechanism of centralising the post-transcriptional processing and storage of various RNA species [40]. Yet, its specific function has remained elusive for decades. One possible function is related to the pluripotency of stem cells and germ cells. Planarians are notorious for their strong regenerative ability. This exceptional property is considered to reside in specific stem cells termed neoblast that contain a chromatoid body [24]. The chromatoid body is also predicted to give germ cells the ability to differentiate while maintaining a totipotent genome [25]. Interestingly, PrP is a marker for hematopoietic stem cells and supports their self-renewal [41]. In addition, PrP positively regulates the proliferation of neural precursors during developmental and adult mammalian neurogenesis [42]. It would be interesting to determine if this proliferation activity of PrP depends on the formation of PrP-RNPs.

PrP-RNPs, like chromatoid bodies share components with cytoplasmic foci termed P bodies where untranslated mRNAs accumulate, awaiting translational reactivation or degradation (Anderson and Kedersha, 2006; Seydoux and Braun, 2006). These components include Dcp1a, and microRNAs. A complete list of molecules for any of these granules is not yet available. Such a list would be essential to determine the relationship between these RNA granules. Although these RNA granules may have a very similar composition, the juxtanuclear localization of PrP-RNPs and chromatoid bodies is specific. Thus, the function of PrP-RNPs and chromatoid bodies is also likely different from the function of P bodies.

### *4.3. PrP and the RNA connection*

It is well established that PrP has nucleic-acid binding activity in vitro [43]. In some instances, PrP exhibits RNA chaperone properties similar to the nucleoprotein NCP7 of HIV-1, and to the nucleoprotein of feline immunodeficiency virus [44, 45]. Reciprocally, binding of recombinant or purified PrP to RNA in vitro induces profound conformational rearrangements and results in a protease-K resistant ($PrP^{Res}$) isoform [46–49]. Furthermore, RNA molecules co-localize with large extracellular hamster prions aggregates in infected hamsters [50]. Thus, it is tempting to propose that interactions between RNA and PrP may be a facilitating if not an essential factor in the conversion of PrP into $PrP^{Res}$.

Our results reveal a novel dimension in the relation between PrP and RNA in vivo. Indeed, a simple interaction of PrP with mRNAs, 5S rRNA, U1 snRNA, tRNA, and several miRNAs, but not with 18S and 28S rRNAs would hardly explain how these RNAs and several proteins involved in the life and death of RNA are specifically concentrated in a large ribonucleoprotein particle. We suggest that a new signalling mechanism between PrP and RNA remains to be discovered.

In summary, the discovery of PrP-RNPs should prove to be extremely useful for better understanding the biological relevance of cytoplasmic PrP.

## Acknowledgments

We thank Dr Leonid Volkov for his expertise with confocal microscopy, and Dr Guylain Boissonneault for sharing with us his expertise in spermatogenesis. We also thank Dr Elisabeth Sztul (University of Alabama at Birmingham, AL USA) for providing the construct encoding GFP-250.

## References

[1] S.B. Prusiner, Prions, Proc. Natl. Acad. Sci. U. S. A. 95 (1998) 13363–13383.
[2] J. Collinge, Prion diseases of humans and animals: their causes and molecular basis, Annu. Rev. Neurosci. 24 (2001) 519–550.
[3] A. Aguzzi, M. Polymenidou, Mammalian prion biology: one century of evolving concepts, Cell 116 (2004) 313–327.
[4] M. Vey, S. Pilkuhn, H. Wille, R. Nixon, S.J. DeArmond, E.J. Smart, R.G. Anderson, A. Taraboulos, S.B. Prusiner, Subcellular colocalization of the cellular and scrapie prion proteins in caveolae-like membranous domains, Proc. Natl. Acad. Sci. U. S. A. 93 (1996) 14945–14949.
[5] C.S. Yost, C.D. Lopez, S.B. Prusiner, R.M. Myers, V.R. Lingappa, Non-hydrophobic extracytoplasmic determinant of stop transfer in the prion protein, Nature 343 (1990) 669–672.

[6] C.D. Lopez, C.S. Yost, S.B. Prusiner, R.M. Myers, V.R. Lingappa, Unusual topogenic sequence directs prion protein biogenesis, Science 248 (1990) 226–229.
[7] R.S. Hegde, J.A. Mastrianni, M.R. Scott, K.A. DeFea, P. Tremblay, M. Torchia, S.J. DeArmond, S.B. Prusiner, V.R. Lingappa, A transmembrane form of the prion protein in neurodegenerative disease, Science 279 (1998) 827–834.
[8] R.S. Stewart, P. Piccardo, B. Ghetti, D.A. Harris, Neurodegenerative illness in transgenic mice expressing a transmembrane form of the prion protein, J. Neurosci. 25 (2005) 3469–3477.
[9] A. Mironov Jr., D. Latawiec, H. Wille, E. Bouzamondo-Bernstein, G. Legname, R.A. Williamson, D. Burton, S.J. DeArmond, S.B. Prusiner, P.J. Peters, Cytosolic prion protein in neurons, J. Neurosci. 23 (2003) 7183–7193.
[10] A. Strom, G.S. Wang, R. Reimer, D.T. Finegood, F.W. Scott, Pronounced cytosolic aggregation of cellular prion protein in pancreatic beta-cells in response to hyperglycemia, Lab. Invest. 87 (2007) 139–149.
[11] Y. Kikuchi, T. Kakeya, O. Nakajima, A. Sakai, K. Ikeda, N. Yamaguchi, T. Yamazaki, K.I. Tanamoto, H. Matsuda, J.I. Sawada, K. Takatori, Hypoxia induces expression of a GPI-anchorless splice variant of the prion protein, FEBS J. 275 (2008) 2965–2976.
[12] H. Ecroyd, P. Sarradin, J.L. Dacheux, J.L. Gatti, Compartmentalization of prion isoforms within the reproductive tract of the ram, Biol. Reprod. 71 (2004) 993–1001.
[13] N.S. Rane, J.L. Yonkovich, R.S. Hegde, Protection from cytosolic prion protein toxicity by modulation of protein translocation, EMBO J. 23 (2004) 4550–4559.
[14] J. Ma, R. Wollmann, S. Lindquist, Neurotoxicity and neurodegeneration when PrP accumulates in the cytosol, Science 298 (2002) 1781–1785.
[15] A.S. Rambold, M. Miesbauer, D. Rapaport, T. Bartke, M. Baier, K.F. Winklhofer, J. Tatzelt, Association of Bcl-2 with misfolded prion protein is linked to the toxic potential of cytosolic PrP, Mol. Biol. Cell 18 (2006) 3356–3368.
[16] X. Roucou, Q. Guo, Y. Zhang, C.G. Goodyer, A.C. LeBlanc, Cytosolic prion protein is not toxic and protects against Bax-mediated cell death in human primary neurons, J. Biol. Chem. 278 (2003) 40877–40881.
[17] L. Fioriti, S. Dossena, L.R. Stewart, R.S. Stewart, D.A. Harris, G. Forloni, R. Chiesa, Cytosolic prion protein (PrP) is not toxic in N2a cells and primary neurons expressing pathogenic PrP mutations, J. Biol. Chem. 280 (2005) 11320–11328.
[18] J. Jodoin, S. Laroche-Pierre, C.G. Goodyer, A.C. LeBlanc, Defective retrotranslocation causes loss of anti-Bax function in human familial prion protein mutants, J. Neurosci. 27 (2007) 5081–5091.
[19] C. Grenier, C. Bissonnette, L. Volkov, X. Roucou, Molecular morphology and toxicity of cytoplasmic prion protein aggregates in neuronal and non-neuronal cells, J. Neurochem. 97 (2006) 1456–1466.
[20] K. Goggin, S. Beaudoin, C. Grenier, A.A. Brown, X. Roucou, Prion protein aggresomes are poly(A)(+) ribonucleoprotein complexes that induce a PKR-mediated deficient cell stress response, Biochim. Biophys. Acta 1783 (2008) 479–491.
[21] N. Kotaja, S. Kimmins, S. Brancorsini, D. Hentsch, J.L. Vonesch, I. Davidson, M. Parvinen, P. Sassone-Corsi, Preparation, isolation and characterization of stage-specific spermatogenic cells for cellular and molecular analysis, Nat. Methods 1 (2004) 249–254.
[22] J.A. Johnston, C.L. Ward, R.R. Kopito, Aggresomes: a cellular response to misfolded proteins, J. Cell. Biol. 143 (1998) 1883–1898.
[23] N. Shibata, Y. Umesono, H. Orii, T. Sakurai, K. Watanabe, K. Agata, Expression of VASA(vas)-related genes in germline cells and totipotent somatic stem cells of planarians, Dev. Biol. 206 (1999) 73–87.
[24] M. Yoshida-Kashikawa, N. Shibata, K. Takechi, K. Agata, DjCBC-1, a conserved DEAD box RNA helicase of the RCK/p54/Me31B family, is a component of RNA-protein complexes in planarian stem cells and neurons, Dev. Dyn. 236 (2007) 3436–3450.
[25] G. Seydoux, R.E. Braun, Pathway to totipotency: lessons from germ cells, Cell 127 (2006) 891–904.
[26] J. Figueroa, L.O. Burzio, Polysome-like structures in the chromatoid body of rat spermatids, Cell Tissue Res. 291 (1998) 575–579.
[27] F. Moussa, R. Oko, L. Hermo, The immunolocalization of small nuclear ribonucleoprotein particles in testicular cells during the cycle of the seminiferous epithelium of the adult rat, Cell Tissue Res. 278 (1994) 363–378.
[28] C.M. Haraguchi, T. Mabuchi, S. Hirata, T. Shoda, K. Hoshi, K. Akasaki, S. Yokota, Chromatoid bodies: aggresome-like characteristics and degradation sites for organelles of spermiogenic cells, J. Histochem. Cytochem. 53 (2005) 455–465.
[29] Y. Toyooka, N. Tsunekawa, Y. Takahashi, Y. Matsui, M. Satoh, T. Noce, Expression and intracellular localization of mouse VASA-homologue protein during germ cell development, Mech. Dev. 93 (2000) 139–149.
[30] N. Kotaja, S.N. Bhattacharyya, L. Jaskiewicz, S. Kimmins, M. Parvinen, W. Filipowicz, P. Sassone-Corsi, The chromatoid body of male germ cells: similarity with processing bodies and presence of Dicer and microRNA pathway components, Proc. Natl. Acad. Sci. U. S. A. 103 (2006) 2647–2652.
[31] H.W. Hwang, E.A. Wentzel, J.T. Mendell, A hexanucleotide element directs microRNA nuclear import, Science 315 (2007) 97–100.
[32] X.M. Chen, P.L. Splinter, S.P. O'Hara, N.F. LaRusso, A cellular micro-RNA, let-7i, regulates Toll-like receptor 4 expression and contributes to cholangiocyte immune responses against *Cryptosporidium parvum* infection, J. Biol. Chem. 282 (2007) 28929–28938.
[33] N. Kedersha, G. Stoecklin, M. Ayodele, P. Yacono, J. Lykke-Andersen, M.J. Fritzler, D. Scheuner, R.J. Kaufman, D.E. Golan, P. Anderson, Stress granules and processing bodies are dynamically linked sites of mRNP remodelling, J. Cell Biol. 169 (2005) 871–884.
[34] N. Cougot, S. Babajko, B. Seraphin, Cytoplasmic foci are sites of mRNA decay in human cells, J. Cell Biol. 165 (2004) 31–40.
[35] A. Wilczynska, C. Aigueperse, M. Kress, F. Dautry, D. Weil, The translational regulator CPEB1 provides a link between dcp1 bodies and stress granules, J. Cell Sci. 118 (2005) 981–992.
[36] S. Chuma, M. Hiyoshi, A. Yamamoto, M. Hosokawa, K. Takamune, N. Nakatsuji, Mouse Tudor Repeat-1 (MTR-1) is a novel component of chromatoid bodies/nuages in male germ cells and forms a complex with snRNPs, Mech. Dev. 120 (2003) 979–990.
[37] M. Parvinen, The chromatoid body in spermatogenesis, Int. J. Androl. 28 (2005) 189–201.
[38] J.L. Silva, L.M. Lima, D. Foguel, Y. Cordeiro, Intriguing nucleic-acid-binding features of mammalian prion protein, Trends Biochem. Sci. 33 (2008) 132–140.
[39] S. Weiss, D. Proske, M. Neumann, M.H. Groschup, H.A. Kretzschmar, M. Famulok, E.L. Winnacker, RNA aptamers specifically interact with the prion protein PrP, J. Virol. 71 (1997) 8790–8797.
[40] N. Kotaja, P. Sassone-Corsi, The chromatoid body: a germ-cell-specific RNA-processing centre, Nat. Rev., Mol. Cell Biol. 8 (2007) 85–90.
[41] C.C. Zhang, A.D. Steele, S. Lindquist, H.F. Lodish, Prion protein is expressed on long-term repopulating hematopoietic stem cells and is important for their self-renewal, Proc. Natl. Acad. Sci. U. S. A. 103 (2006) 2184–2189.
[42] A.D. Steele, J.G. Emsley, P.H. Ozdinler, S. Lindquist, J.D. Macklis, Prion protein (PrPc) positively regulates neural precursor proliferation during developmental and adult mammalian neurogenesis, Proc. Natl. Acad. Sci. U. S. A. 103 (2006) 3416–3421.
[43] D. Marc, R. Mercey, F. Lantier, Scavenger, transducer, RNA chaperone? What ligands of the prion protein teach us about its function, Cell. Mol. Life Sci. 64 (2007) 815–829.
[44] C. Gabus, E. Derrington, P. Leblanc, J. Chnaiderman, D. Dormont, W. Swietnicki, M. Morillas, W.K. Surewicz, D. Marc, P. Nandi, J.L. Darlix, The prion protein has RNA binding and chaperoning properties characteristic of nucleocapsid protein NCP7 of HIV-1, J. Biol. Chem. 276 (2001) 19301–19309.
[45] M. Moscardini, M. Pistello, M. Bendinelli, D. Ficheux, J.T. Miller, C. Gabus, S.F. Le Grice, W.K. Surewicz, J.L. Darlix, Functional interactions of nucleocapsid protein of feline immunodeficiency virus and cellular prion protein with the viral RNA, J. Mol. Biol. 318 (2002) 149–159.
[46] V. Adler, B. Zeiler, V. Kryukov, R. Kascsak, R. Rubenstein, A. Grossman, Small, highly structured RNAs participate in the conversion of human recombinant $PrP^{Sen}$ to $PrP^{Res}$ *in vitro*, J. Mol. Biol. 332 (2003) 47–57.
[47] N.R. Deleault, R.W. Lucassen, S. Supattapone, RNA molecules stimulate prion protein conversion, Nature 425 (2003) 717–720.
[48] P.K. Nandi, J.C. Nicole, Nucleic acid and prion protein interaction produces spherical amyloids which can function in vivo as coats of spongiform encephalopathy agent, J. Mol. Biol. 344 (2004) 827–837.
[49] N.R. Deleault, B.T. Harris, J.R. Rees, S. Supattapone, Formation of native prions from minimal components in vitro, Proc. Natl. Acad. Sci. U. S. A. 104 (2007) 9741–9746.
[50] J.C. Geoghegan, P.A. Valdes, N.R. Orem, N.R. Deleault, R.A. Williamson, B.T. Harris, S. Supattapone, Selective incorporation of polyanionic molecules into hamster prions, J. Biol. Chem. 282 (2007) 36341–36353.
[51] R. Zahn, A. Liu, T. Lührs, R. Riek, C. von Schroetter, F. López García, M. Billeter, L. Calzolai, G. Wider, K. Wüthrich, NMR solution structure of the human prion protein, NMR solution structure of the human prion protein, Proc. Natl. Acad. Sci. U. S. A. 97 (2000) 145–150.